

In silico and *in vitro* Investigation of Osteogenesis Potentiality of *Smilax china* Hydro Alcoholic Root Extract on Human Osteoblast-like Cell Line (Saos2)-A Novel Approach

Hafiz A. Makeen¹, Mohammed Albratty^{2,*}

¹Pharmacy Practice Research Unit, Department of Pharmacy Practice, College of Pharmacy, Jazan University, Jazan, SAUDI ARABIA.

²Department of Pharmaceutical Chemistry and Pharmacognosy, College of Pharmacy, Jazan University, Jazan, SAUDI ARABIA.

ABSTRACT

Background: Osteoporosis is a skeletal illness characterised by the breakdown of bone tissue's micro-architecture, which increases the risk of fractures by making bones more brittle. Nowadays, the herbal based therapies gaining more attraction towards osteoporosis for its low risk of side effects. **Aim:** The goal of this study is to prove *Smilax china* root extract's osteogenesis ability towards osteoblast like cell line Saos2. **Materials and Methods:** Cytotoxicity parameters such as tetrazolium-based assay (MTT), Trypan Blue Exclusion (TBE) and morphometric analysis were used to assess its anti-apoptotic nature and dose fixation. The cells were differentiated using Osteogenic Differentiation Media (ODM), then alkaline phosphatase and Alizarin red staining were performed. Molecular docking was performed for the interaction of rutin and quercetin with Runx1 and runx2 by Auto dock vina. **Results:** Cytotoxicity assessments revealed that the *Smilax china* root extract showed 100% viability up to 200 µg/mL. Same results were obtained in trypan blue based viability test and morphometric analysis. Alkaline phosphatase and mineralisation were increased gradually at 50, 100 and 200 µg/mL of *Smilax china* root extract treated cells as dose dependent manner. *In silico* analysis revealed strong binding affinities of quercetin and rutin with Runx1 and Runx2 (Quercetin - Runx1 - (-7.9), Quercetin - Runx2 - (-7.4), Rutin - Runx1 - (-8.5) and Rutin - Runx2 - (-7.9)) suggesting their potential involvement in osteogenic regulation, although drug-likeness screening indicated the need for further optimization. **Conclusion:** He findings suggest that *Smilax china* root extract promotes osteogenic differentiation in Saos-2 cells and that its bioactive compounds may interact favorably with osteogenic transcription factors. Further studies are warranted to validate its therapeutic potential as a safe herbal candidate for osteoporosis management.

Key words: Alkaline phosphatase, Mineralisation, Osteogenesis, Osteoporosis, Saos2 cells, *Smilax china*.

Correspondence:

Mohammed Albratty

Department of Pharmaceutical Chemistry and Pharmacognosy, College of Pharmacy, Jazan University, Jazan, SAUDI ARABIA.

Email: malbratty@jazanu.edu.sa

Received: 28-11-2025;

Revised: 19-12-2025;

Accepted: 09-02-2026.

INTRODUCTION

Osteoporosis, which increases bone fragility, is characterised by decreased bone mass and micro architecture of the bone tissue degradation.¹ The disease often presents clinically with a fracture as its initial symptom. Osteoporosis - a complex, chronic, progressive illness which is the most prevalent metabolic bone disease globally. It has been found to be most common in the elderly, weak bone skeletal structures, post-menopausal women and persons of all ages. Over 200 million people worldwide are thought to have osteoporosis in recent times.² The International Osteoporosis Foundation has released statistics showing that

1 in 5 men and 1 in 3 women over 50 ages may suffer with an osteoporotic fracture.³ Bone development relies on various biological factors and processes, one of which is the transcription of bone-specific genes.⁴ Genetic factors, oxidative stress, cellular ageing, inflammation, and estrogen deficiency are cited as the causative of osteoporosis. RANKL inhibitors, bisphosphonates, PTH analogues, anti-sclerostin antibodies, hormone therapy, calcitonin, and other treatments are preferred based on the underlying cause, but they come with a plethora of negative effects.⁵ Herbal medicines have minimal to no side effects and can be used as a substitute to help overcome the effects of the current course of therapy. Many studies have proven that the phytochemicals found in plants such as poly phenols, flavonoids, alkaloids, saponins etc., do tremendous pharmacological beneficial to the mankind. Here in this study, *Smilax china* (SC) root extract was chosen to investigate for its osteogenic potency.

Smilax China is referred as "Bilri," in Pakistan and "Ba Qia" (or "Jin Gang Teng") in China. There are 350 species of *Smilax*,



DOI: 10.5530/ijper.20263810

Copyright Information :

Copyright Author (s) 2026 Distributed under Creative Commons CC-BY 4.0

Publishing Partner : Manuscript Technomedia. [www.mstechnomedia.com]

and they are found worldwide in both tropical and temperate climates, primarily in East Asia and North America.^{6,7} The rhizome of the *Smilax* genus is well recognised to possess a variety of pharmacological properties. Numerous studies discuss the anti-bacterial, anti-mutagenic, anti-oxidant, anti-inflammatory, anti-cancer, and neuroprotective properties of *S. china*.^{7,8}

Previous studies have demonstrated the presence of alkaloids, steroidal saponins such as dioscin, flavonoids such as rutin, astilbin and engeletin, and phenolic acids such as caffeic acid, gentisic acid, and trans-o-coumaric acid in the rhizome of SC.⁹ According to earlier research, flavonoids and polyphenols decrease RANKL-mediated osteoblastogenesis, which is significant for osteoblast growth.^{10,11} Astilbin, a flavonoids found in the root extract of *Smilax glabra*, was studied and shown to have osteoblastogenic properties against the Saos2 cell line.¹² *S. china* tubers also contain the highly-profile phytochemicals mentioned above. Studies further reveal that its strong anti-oxidant content shields body cells from oxidative damage while its anti-inflammatory qualities treat gout and rheumatoid arthritis.^{13,14} the impact of its extensive phytochemical profile on osteogenesis has not been studied or supported by data. Thus, in light of these conditions, an *in vitro* study of the hydroalcoholic extract of SC root extract was conducted using the Saos2 cell line. This study focuses on the role of Runx family transcription factors in osteogenesis, particularly Runx1 and Runx2, which are known to regulate osteogenic gene transcription and investigated the binding potential of two active components from *Smilax china*, quercetin and rutin¹⁵ with Runx1 and Runx2 using *in silico* molecular docking. Additionally, we assessed gramine for drug likeliness, toxicity, and bioactivity to evaluate its potential as a therapeutic agent.

MATERIALS AND METHODS

Preparation of hydro alcoholic extract

Hydro alcoholic extract preparation method was followed by the protocol suggested by Iqbal *et al.*, 2023 with slight modification.¹⁶ *Smilax china* root was collected and cut into small pieces. The cut and washed pieces was dehydrated under sunshade. Dried root pieces of *Smilax china* were added into mixture of ethanol and water as 70:30 ratio for the extraction of hydro alcoholic extract for 48 hr with continues stirring. The extracted content was filtered through Whatman filter paper No.1. The filtrate liquid was collected in a petri dish and dried under 40°C for 48 hr. The dried powder was collected, weighed and stored for future analysis.

In vitro Analysis

Cell culture

Osteosarcoma cell line (Saos2) was purchased from ATCC, USA. The cells were grown using 10% Dulbecco's modified eagles'

medium with fetal bovine serum containing 1% penicillin/streptomycin antibiotic. The cells were incubated in 37°C with 5% CO₂. The cells were subcultured for further analysis once it reached 70-80% confluency.

Anti-apoptotic property

Cytotoxicity analysis

Cytotoxicity analysis protocol was performed by the protocol given by Mosmann, 1983.¹⁷ Cells were seeded in 96 well plates as 5000 cells per well and incubated at 37°C in CO₂ incubator to reach the confluency up to 70 - 80% for 48 hr. Then, the media was aspirated and hydroalcoholic extract of *Smilax china* root powder (SCR-HAE) was added as different concentration ranging from 0.2 - 600 µg/mL and untreated well-kept as control. The treated plate was incubated for 24 - 48 hr. Then the effect was noticed and photographed under phase contrast microscope. Later, the drug from each well was removed and replaced with 2% media containing 5 mg/mL of MTT reagent in dark and incubated the plate at appropriate condition for 4 hr. The media with MTT was aspirated and the attached formazan crystal was diluted with DMSO. Then the samples were taken for UV reading at 490 and 630 nm.

TBE Assay (Trypan Blue Exclusion)

The cytotoxicity results were further analysed with TBE assay¹⁸ for the dose fixation. For this the treated and untreated cells were trypsinized using Trypsin EDTA. The cell pellet obtained from centrifugation was mixed with 1 mL of media and the pellet was re-suspend. From the suspension, cells of small volume were taken and mixed with equal volume of Trypan blue staining solution. 10 µL of sample were added into hemocytometer and the viable and dead cells were counted under Phase contrast microscopy. The percentage of viable and non-viable cells were calculated using following formula,

$$\% \text{ viability} = \frac{\text{Number of viable cells}}{\text{Number of total cells}} \times 100$$

Morphometric analysis

The required numbers of cells such as 1x10⁵ cells/well were seeded in 6 well plates and incubated for appropriate confluency. Then, the grown cells were treated with 100, 200, 300, 400 and 500 µg/mL. Untreated cells used as control. The cell structure was observed at 24 hr after the treatment and photographed under phase contrast microscopy (Optika, Italy) as per the protocol suggested by Chen *et al.*, 2018.¹⁹

Osteogenesis property

Alkaline phosphatase quantitative and alizarin red quantitative, qualitative analysis was performed based on the protocol prescribed by Mahendiran *et al.*, 2022 with little modification.²⁰

Alkaline Phosphatase assay

Since alkaline phosphatase enzyme is generated in the early stages of bone formation, it is referred to as an early marker and is considered the most significant parameter in osteogenesis. For the estimation of ALP, the cells of 1×10^5 were seeded in 6 well plates and incubated. The cells were subjected to osteogenic differentiation for 7 days with Osteogenic Differentiated Media (ODM) as mentioned previously. The cells were treated with 50, 100 and 200 $\mu\text{g}/\text{mL}$ of SCR-HAE and the untreated kept as control. The treated cells were washed thrice with Phosphate buffered saline (pH 7.4). In order to release the ALP from the cells, it was treated with lysis buffer contains Glycine 0.1 M, MgCl_2 1 mM, Triton X-100 1% in PBS solution (pH 10.5). 0.5 mL/ well of lysis buffer was added and incubated for 60 min at room temperature. Then, the 100 μL of lysate was mixed with 250 μL of pNPP (1 mg/mL) substrate and incubated at 37°C for 30 min. After that, the samples were put in an ice bath at 0°C with 50 μL of 3N NaOH solution to stop the reaction. Subsequently, a Biotek ELX 800 microplate reader was used to read the collected solution at 405 nm. Three duplicate runs of the samples were performed, and the average results were calculated.

Alizarin Red staining Assay

One other important osteogenesis-related metric is the estimation of calcium deposition. It was termed a "late marker in osteogenesis" because mineralization typically occurred during the later phases of the formation of the bone matrix. The cells were differentiated using ODM medium for up to 14 days, with frequent media changes on the requirement basis, in order to estimate the calcium accumulation present. At the end of the experiment, the cells were treated with SCR-HAE as 50, 100 and 200 $\mu\text{g}/\text{mL}$ Untreated cells maintained as control. The treated and control cells were rinsed three times with PBS solution (pH 7.4) and fixed with 4% (v/v) formaldehyde at room temperature for 15 min. Next, the cells were stained with 2% ARS solution (pH 4.2) for 15 to 30 min at room temperature in the dark. The cells were stained, then twice-washed in distilled water before being examined using a bright field microscope (Optika, Italy) for qualitative images. To do a quantitative measurement, 800 μL of 10% (v/v) acetic acid was added to the bound ARS, and incubated for 30 min at room temperature with gentle agitation. Using a microplate reader (Biotek - ELX 800), the absorbance at 430 nm was used to read the ARS. Three copies of each sample were examined and values provided as triplicated.

Table 1: Showed the scores obtained from the analysis of Lipinski's rule of five, Drug likeliness, Bioactive and ADMET.

Lipinski's Rule of five									
Compounds	Topological Polar Surface Area (\AA)	MW (<500)	Heavy atom count (natoms)	Hydrogen bond donors (nOHNH) (≤ 5)	Hydrogen bond acceptors (nON) (≤ 10)	Rotatable bonds (nrotb) (≤ 10)	Lipinski Violations		
Quercetin	131.36	302.24	16	5	7	1	0		
Rutin	269.43	610.52	16	10	16	6	3		
Drug Likeliness									
Compounds	Drug Likeliness	Mutant	Tumorigenic	Reproductive Effect	Irritant				
Quercetin	3.075	None	None	None	None				
Rutin	1.9337	None	None	None	None				
Bioactivity									
Compounds	GPCR ligand	Ion channel modulator	Kinase inhibitor	Nuclear receptor ligand	Protease inhibitor	Enzyme inhibitor			
Quercetin	-0.06	-0.19	0.28	0.36	-0.25	0.28			
Rutin	-0.05	-0.52	-0.14	-0.23	-0.07	0.12			
ADMET									
Compounds	Consensus Log Po/w	BBB	P-gp Substrate	CYP1A2 inhibitor	CYP2C19 inhibitor	CYP2C9 inhibitor	CYP2D6 inhibitor	CYP3A4 inhibitor	Log Kp
Quercetin	1.23	No	No	Yes	No	No	Yes	Yes	-7.05 cm/s
Rutin	-1.29	No	Yes	Yes	No	No	No	No	-10.26 cm/s

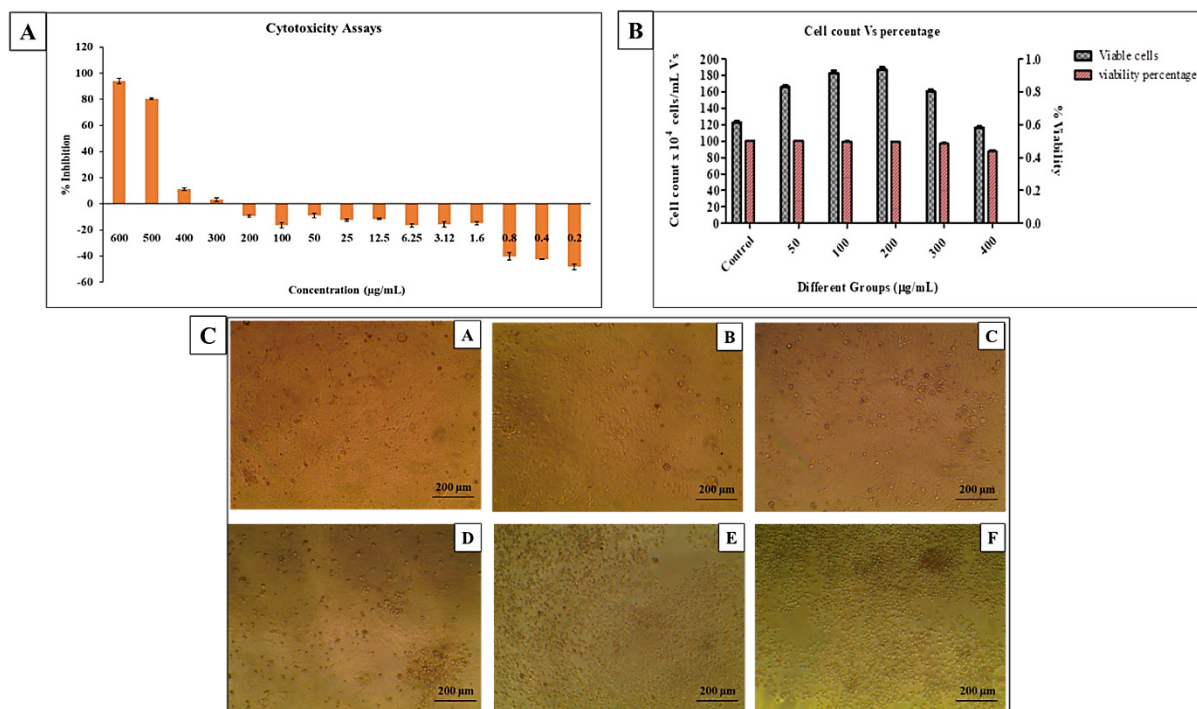


Figure 1: A: MTT assay. Cytotoxicity analysis of SCR-HAE against Saos2 cell line which showed the safer range up to 200 µg/mL. B: TBE assay. Viability analysis of SCR-HAE against Saos2 cell line. Graph showed based on the drug dosage up to 200 µg/mL the viability was stable and started decreasing from 300 µg/mL. C - Morphometric analysis. In C: A: control - showed fine morphology, B: 100 µg/mL, C: 200 µg/mL - showed distinct morphology, D: 300 µg/mL, E: 400 µg/mL, F: 500 µg/mL - showed morphological deterioration based on dosage dependent.

In silico Analysis

Acquisition of 3D Structures of Proteins and Ligands

The 3D structures of quercetin and rutin were retrieved from the PubChem database in sdf format and converted to pdbqt format using PyMOL software. The crystal structures of RUNX1 (PDB ID: 4LOY, chain A, 2.50 Å resolution) and RUNX2 (PDB ID: 6VGE, chain A, 4.25 Å resolution) were obtained from the RCSB Protein Data Bank. All water molecules and hetero atoms were removed, and the proteins were prepared using standard docking protocols before performing molecular docking with quercetin and rutin.

Molecular Docking

We determined the binding affinities of quercetin and rutin with Runx1 and Runx2 proteins using Autodock Vina. The 2D structures of the active components were obtained from PubChem. Protein and ligand preparations were completed with MGL Autodock tools and saved in PDBQT format. Docking was performed with grid dimensions of 96x96x96 Å and 0.375 Å spacing. Autodock Vina was executed via the command prompt to obtain binding affinities. Binding configurations and interactions were visualized using Accelrys BIOVIA Discovery Studio 2017 R2 and PyMOL.

Prediction of Activity Spectra for Substances

Lipinski's Rule of Five was assessed the drug-likeness of the active molecules based on their physicochemical properties using Lipinski's Rule of Five, with evaluations performed via the Molinspiration online tool (<https://www.molinspiration.com/>).

Drug Likeliness and Toxicity

Drug-likeness and toxicity were evaluated using OSIRIS Data Warrior software, which provides scores and details on mutagenicity, carcinogenicity, reproductive effects, and irritancy.

Bioactivity Score

Bioactivity scores, indicating the compound's potential to function as a drug without disturbing normal physiological functions, were calculated using Molinspiration (<https://www.molinspiration.com/>). Scores above 0.000 indicate bioactivity, scores between -0.50 and 0.00 suggest moderate activity, and scores below -0.50 are considered biologically inactive.

ADMET Analysis

The pharmacokinetic parameters of Adsorption, Distribution, Metabolism, Excretion, and Toxicity (ADMET) were evaluated using the Swiss ADME online tool (<http://www.swissadme.ch/index.php>). This included assessing skin permeability, lipophilicity, tissue absorption, and metabolic inhibition.

Statistical Analysis

The assays were triplicates and the result outcomes were given as Mean±SD. The values were analysed for statistical comparison using GraphPad PRISM 5.1. The values were subjected to one way ANOVA and the groups were compared using Turkey's multiple comparison test. $p=0.0001$ considered as significant.

RESULTS

In vitro Analysis

Anti-apoptotic property

Cytotoxicity analysis, TBE assay and morphology assessment

The cytotoxicity analysis of SCR-HAE against Saos2 cell line was assessed. Figure 1A showed the cytotoxicity analysis of SCR-HAE in the range between 0.2 - 600 µg/mL. From the figure it was understood that there was no inhibition was found up to 200 µg/mL. From 300 µg/mL inhibition was initiated and increased gradually based on dosage. 500 and 600 µg/mL showed maximum inhibition as 80.45 ± 0.71 and 93.94 ± 1.88 respectively. From the analysis it was confirmed that up to 200 µg/mL SCR-HAE was considered as safer range. The dosage for osteogenesis analysis fixed as 50, 100 and 200 µg/mL and this result was further rechecked with TBE assay. TBE assay was performed for 50, 100,

200, 300 and 400 µg/mL which also showed 100% viability at 50, 100 and 200 µg/mL. 300 and 400 µg/mL showed 96.60 ± 1.17 and 87.31 ± 1.59 respectively which was depicted in Figure 1B. The morphometric analysis was depicted in Figure 1C which showed deformation of cells at 300, 400 and 500 whereas 100 and 200 µg/mL showed regular cell morphology as like control group. So, the morphology analysis also corroborates the results of cytotoxicity and TBE assays. Finally, the safer range dosage such as 50, 100 and 200 µg/mL was carried forward for the further assays to evaluate its osteogenesis ability.

Osteogenesis Property

Alkaline phosphatase assay

Alkaline phosphatase enzyme release was analysed for SCR-HAE treated Saos2 differentiated cells. Figure 2A showed the ALP release at OD 405 nm. From the graph it was observed that there was gradual increase in enzyme release. Control showed 2.857 ± 0.069 whereas treated groups showed 2.956 ± 0.025 , 3.149 ± 0.022 and 3.217 ± 0.05 for 50, 100 and 200 µg/mL respectively. The statistical analysis revealed that 50 µg/mL showed non-significant with control group whereas 100 and 200 µg/mL was highly significant with p value of 0.0001. Saos2 cells differentiated for 7 days and treated with SCR-HAE showed the moderate increase in Alkaline phosphatase enzyme release.

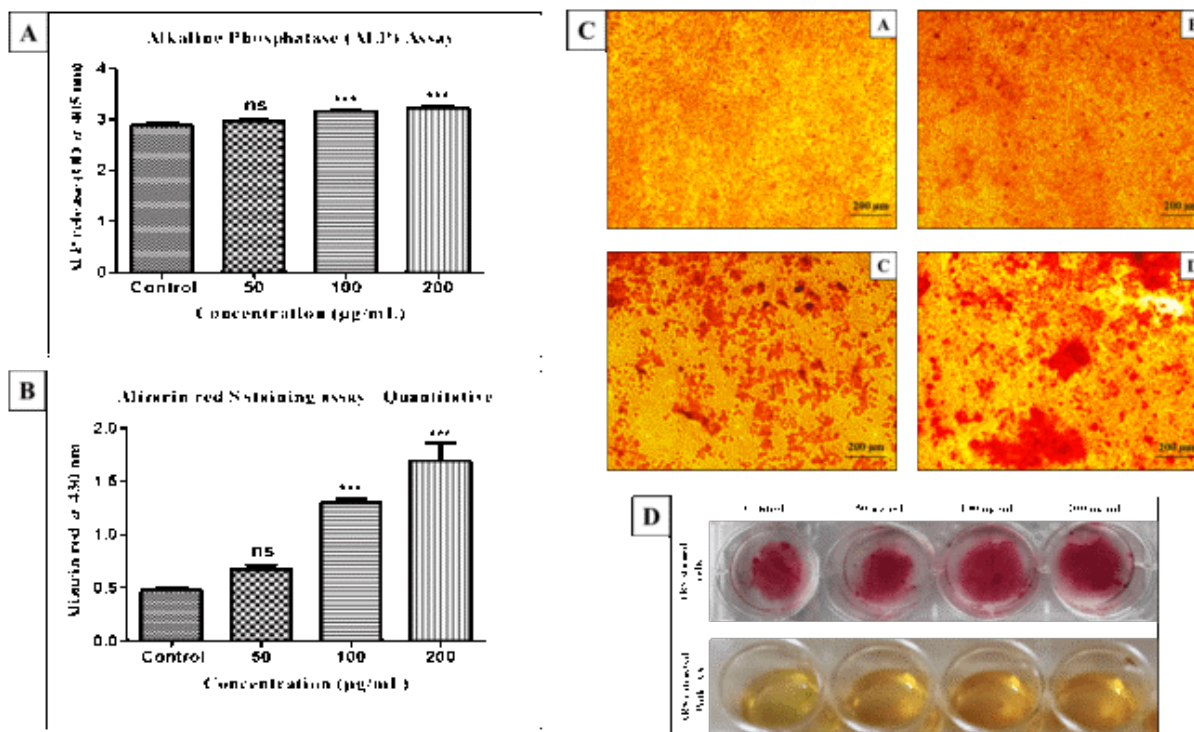



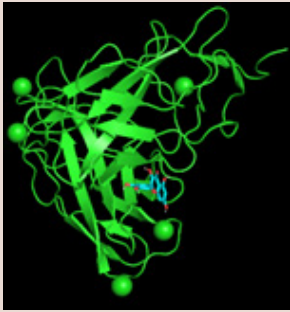


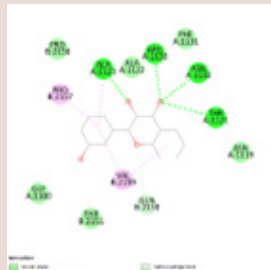

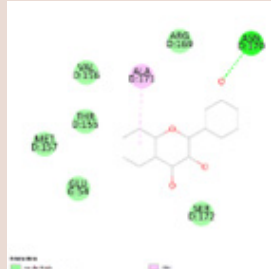
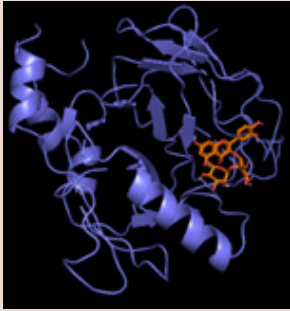
Figure 2: A: ALP quantitative analysis. Graph showed the ALP quantitative assessment for different dosages 50, 100 and 200 µg/mL showed the increasing absorbance based on dosage. B: ARS quantitative analysis. Graph showed the extracted alizarin red from the assay showed 50, 100, 200 µg/mL and control which increased gradually as dose dependent manner. C: ARS qualitative Analysis. The images indicate A: control, B: 50 µg/mL, C: 100 µg/mL and D: 200 µg/mL. From the images the increasing ARS indicates the gradual increase of calcium deposition based on dosage. D: ARS extracted images. Acetic acid extracted ARS images also showed the gradual increase of ARS accumulation.

Alizarin Red S Assay - Quantitative and Qualitative

Calcium deposition in bone matrix mineralisation was one of the prominent steps. Alizarin Red staining assay was performed to check the calcium availability in different dosages of SCR-HAE treated differentiated Saos2 cells. For the mineralisation study the cells were differentiated for 14 days and the Figures 2B-2D showed quantitative and qualitative output of calcium deposition respectively. Figure 2B showed control as 0.473 ± 0.028 , treated groups showed 0.670 ± 0.042 , 1.297 ± 0.043 and 1.697 ± 0.163 for

50, 100 and 200 $\mu\text{g/mL}$ respectively. Statistical analysis showed low dose was non-significant with control. 100 and 200 $\mu\text{g/mL}$ was highly significant with control indicated with ***, where $p < 0.0001$. From the results of quantitative it was clear that the calcium deposition was found increased as dose dependent manner. Qualitative analysis also proved the similar results (Figure 2C) such as control showed no ARS-stained patches where as in treated groups it increased according to the increase in dosages confirming calcium deposition. The stain extracted images (Figure 2D) also proven the similar pattern of increasing.

Table 2: Denotes the cumulative *in silico* results of interaction between quercetin and rutin with Runx1 and Runx2 respectively as 2D and 3D structure.

Ligand	Protein	BE (kcal/mol)	2D structure	3D Structure
Quercetin	Runx1	-7.9		
Quercetin	Runx2	-7.4		
Rutin	Runx1	-8.5		
Rutin	Runx2	-7.9		

The results outcome discloses that the SCR-HAE has the osteogenic potency.

In silico Analysis

Molecular Docking

Molecular docking results showed that both quercetin and rutin had strong binding affinities with Runx1 and Runx2, as detailed in Table 1. Visualization of the binding interactions shown in Figures 3A,3B, Figures 4A,4B confirmed that both compounds formed both polar and non-polar bonds with the target proteins such as Runx1 and Runx2 respectively, supporting their potential impact on osteogenesis via transcription regulation (Table 2).

Prediction of Activity Spectra for Substances

Lipinski's Rule of Five

Quercetin adhered to all aspects of Lipinski's Rule, suggesting it is a suitable candidate for drug development. In contrast, rutin violated three of Lipinski's rules, indicating that further evaluation is needed to assess its drug formulation potential.

Drug Likelihood and Toxicity

OSIRIS Data Warrior analysis indicated that quercetin had a lower drug-likeness score and showed mutagenic and tumorigenic properties, while rutin had a favourable drug-likeness score and no adverse physiological effects.

Bioactivity Score

Quercetin exhibited at least moderate bioactivity across various activities, including GPCR ligand and enzyme inhibition. Rutin also showed at least moderate bioactivity in most categories, except ion channel modulation.

ADMET Analysis

Both compounds demonstrated favourable ADMET properties, with good lipophilicity and absorption characteristics. However,

both compounds had low skin permeability, particularly rutin, which had a skin permeability of -10.26 cm/s, indicating poor skin excretion. Neither compound was able to cross the Blood-Brain Barrier, reducing the risk of neurological effects. Quercetin was found to inhibit three cytochromes, while rutin acted as a P-gp substrate and inhibited cytochrome CYP1A2.

DISCUSSION

Bone - serves as a centre for mineral homeostasis and is an elastic, dynamic connective tissue. Osteogenesis, also known as bone production, is a multi-phase process that starts with mesenchymal stem cell proliferation and ends with the cells' differentiation into pre-osteoblast. Following their maturation into osteoblast, these pre-osteoblasts produce extracellular matrix proteins that aid in the mineralization of bone. Osteoporosis is caused by high bone turnover along with a decrease in bone mass. According to statistics, Asia will account for over half of all osteoporotic fractures by 2050.²¹ Considering the drawbacks of current treatments, plant-derived remedies present a promising, gentle, and cost-friendly approach to tackling this condition, potentially offering a more tolerable and effective solution. In this study we demonstrated *Smilax china* root extract, which is well known plant for its greater anti-oxidant and anti-inflammatory potentiality to investigate its osteogenesis property against osteoblast like cell line (Saos2).SC rhizome owns high profile of various phytochemicals such as flavonoids - astilbin, rutin, engeletin, isoastilbin, cinchonainIa, quercetin-3-O-a-L-rhamnopyranoside and chlorogenic acid,⁸ phenolic acids - Gallic acid, Epigallocatechin, Catechin, Chlorogenic acid, Epicatechin, Epigallocatechin gallate and Epicatechin gallate etc.,⁶

Since many pharmaceutical chemicals and crude plant extracts have been proven to have harmful side effects, our initial goal was to determine cytotoxicity property of SCR-HAE on Saos2 cell line. MTT assay, trypan blue exclusion assay, and morphological analysis were performed to explore its cytotoxic nature. The

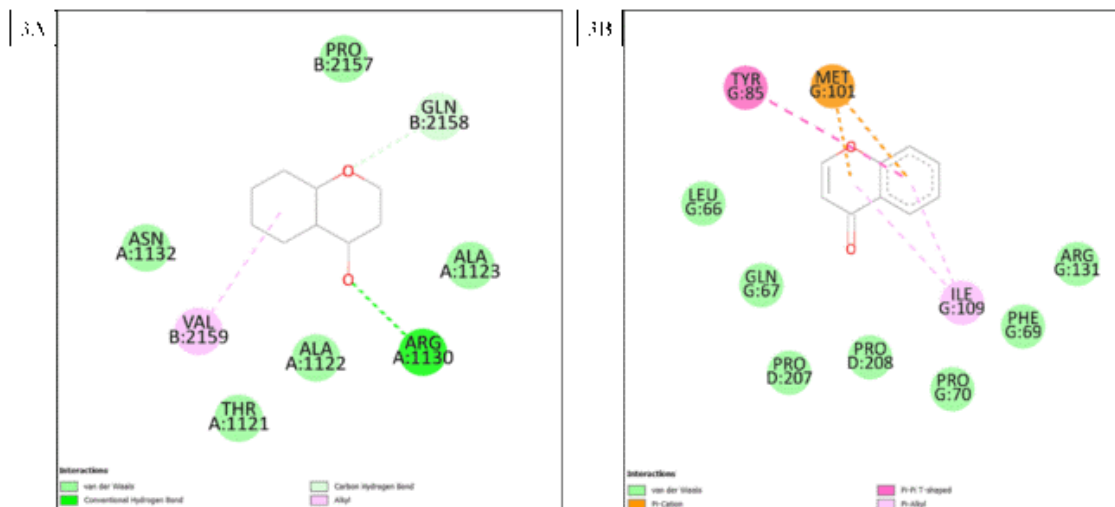


Figure 3: A and B Shows the interaction of quercetin with Runx1 and Runx2 respectively.

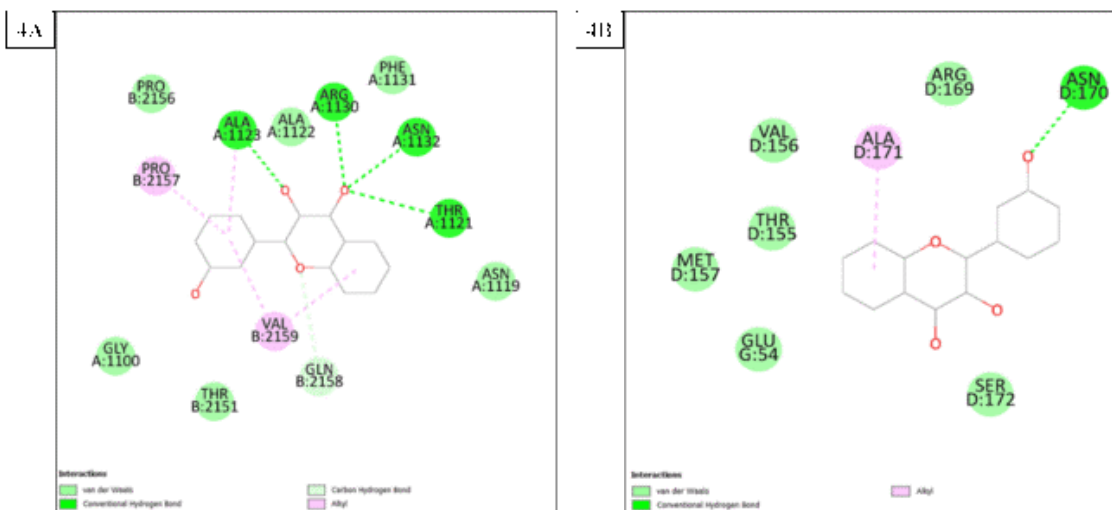


Figure 4: A and B Shows the interaction of rutin with Runx1 and Runx2 respectively.

findings indicated that SCR-HAE has a beneficial effect on cell proliferation, as osteoblastic cells remain unaffected by the extract up to 200 $\mu\text{g}/\text{mL}$ these outcomes suggested that SCR-HAE acted as anti-apoptotic candidate and can be further taken for the osteogenesis analysis. According to a study done on mice by A. Vijayalakshmi *et al.*, 2011, a maximum dosage of 2 g/Kg of SC extract did not result in any behavioural abnormalities or mortality. Therefore, even at large doses, the SC extract was found to have few or no harmful effects.^{22,14}

Alkaline phosphatase is the preliminary marker in the process of osteoblast cell differentiation. During the process of conversion of pre osteoblastic cells into bone cells the release of phosphate occurs. ALP release was estimated for the SCR-HAE treated differentiated cells, which showed the increased ALP release at 7 days of treatment. ALP increase based on the dosage manifested that the bone formation takes place significantly with the support of SCR-HAE. Similarly, the late marker such as calcium was determined using ARS assay. The qualitative and quantitative both the results showed the increasing pattern of mineralization as dose dependent manner at 14th day of analysis.

The main component of bone endocrinology is Osteocalcin (OCN), which is released only by osteoblasts. According to recent reports, osteocalcin, a marker protein of osteoblast growth, has a variety of roles in the body, including the formation of neurones, male fertility, and glucose metabolism. The MAPK3 protein primarily facilitates the expression of osteocalcin by binding to its promoter through its connection with RUNX2.²³ Research indicates that ALP stimulates extracellular mineralisation by releasing inorganic phosphate from inorganic pyrophosphate, which is a mineralisation inhibitor. Calcium and inorganic phosphate buildup triggers mineralisation, which is then followed by crystal growth most notably, the formation of crystalline hydroxyapatite.²⁴

According to the earlier studies, phytochemicals found in plants are the primary factor responsible for the development of bone matrix mineralisation. Flavonoids, in particular, have an impact on MSCs' capacity to self-renew and differentiate into osteogenic tissues by modulating multiple signalling pathways, such as the ERK, PI3K/Akt, and Wnt/ β -catenin pathways. They also control transcription factors and indicators that are particular to bone, including Osx, Runx2, BMP-2, Cbfa1, and ALP.²⁵ According to Lue *et al.*, 2021 Rutin^{26,27} and quercetin²⁶ promotes osteogenic differentiation and inhibit osteoclast activation in MC3T3 E1 cells and bone marrow stromal cells respectively. Similarly, flavanoid Astilbin isolated from *Smilax glabra* rhizome exhibited osteogenesis activity which relatively confirms osteogenic ability of *Smilax china*.¹² earlier researches have been demonstrated that Quercetin stimulates osteogenesis by RANKL, SMAD-dependent, Nrf2, Wnt, and NF- κ B pathway.^{26,28} Similarly, Rutin offers a novel approach to osteoporosis treatment by controlling the FNCD1 (fibronectin type III domain-containing protein) level and autophagy via the Akt/mTOR signalling pathway.^{29,27}

Our experimental findings indicated that *S. china* extract can induce osteogenesis. *In silico* molecular docking confirmed that quercetin and rutin interact strongly with Runx1 and Runx2, suggesting a mechanism of action through transcriptional regulation of osteogenic genes. These results are in par with previous studies conducted by Triwardhani *et al.*, 2023³⁰ for quercetin and rutin's ability to bind with Runx2, confirming our findings. Despite these findings, the potential of these compounds as therapeutic drugs is limited. Rutin's violation of Lipinski's rules and quercetin's potential carcinogenicity raise concerns for drug development. Both compounds exhibited good bioactivity, but their ADMET profiles suggest challenges in metabolic processing. Overall, while the data support the hypothesis that *S. china* extract enhances osteogenesis by modulating transcription factors, further extensive studies are needed to determine the viability of these compounds as drugs for osteogenesis.

CONCLUSION

In summary, our work discloses novel osteogenic potential of SCR-HAE treated in Saos2 osteoblast cells. The extract showed less or negligible inhibition towards Saos2 cells which proved its anti-apoptotic activity. SCR-HAE treated groups exhibited increased ALP activity and mineralization of bone matrix manifested its osteogenic potency which was further cross checked with *in silico* studies. *In silico* findings revealed that quercetin and rutin showed exact bonding with the Runx1 and Runx2 transcriptional factors. Although *Smilax china* root extract poses osteogenic property, more investigation is required to prove therapeutic efficacy.

ABBREVIATIONS

IC₅₀: Half-Maximal Inhibitory Concentration; **DMEM**: Dulbecco's Modified Eagle Medium; **MTT**: 3-(4,5-Dimethylthiazol-2-yl)-2,5-Diphenyltetrazolium Bromide; **DMSO**: Dimethyl sulfoxide; **ODM**: Osteogenic Differentiation Medium; **TBE**: Trypan Blue Exclusion; **PBS**: Phosphate-Buffered Saline; **ALP**: Alkaline Phosphatase; **ADMET**: Absorption, Distribution, Metabolism, Excretion, and Toxicity; **OCN**: Osteocalcin.

CONFLICT OF INTEREST

The authors declare that there is no conflict of interest.

SUMMARY

- *Smilax china* root extract was evaluated for osteogenic potential using SaOS-2 osteoblast-like cells.
- Cytotoxicity assays (MTT, Trypan Blue, morphometric analysis) confirmed 100% cell viability up to 200 µg/mL.
- The extract significantly enhanced alkaline phosphatase activity and matrix mineralization in a dose-dependent manner.
- Molecular docking revealed stable interactions of quercetin and rutin with Runx1 and Runx2 transcription factors.
- In conclusion *Smilax china* root extract promotes osteoblast growth and differentiation indicating osteogenic potential. Though it has been proven *in vitro* studies further in-depth *in vivo* studies are required.

REFERENCES

1. Tasadduq R, Gordon J, Al-Ghanim KA, Lian JB, Van Wijnen AJ, Stein JL, et al. Ethanolic extract of *Cissus quadrangularis* enhances osteoblast differentiation and mineralization of murine pre-osteoblastic MC3T3-E1 cells. *J Cell Physiol*. 2017;232(3):540-7. doi: 10.1002/jcp.25449, PMID 27264191.
2. Zhang X, Wang Z, Zhang D, Ye D, Zhou Y, Qin J, et al. The prevalence and treatment rate trends of osteoporosis in postmenopausal women. *PLOS One*. 2023;18(9) (September 9):e0290289. doi: 10.1371/journal.pone.0290289, PMID 37751427. IOF. Osteoporosis; 2024. Available from: <https://www.osteoporosis.foundation/patient-s/about-osteoporosis>.
3. Kirkham GR, Cartmell SH. Genes and proteins involved in the regulation of osteogenesis. *Genes Osteogenesis*. 2007;3(0):1-22.
4. Zhivodernikov IV, Kirichenko TV, Markina YV, Postnov AY, Marlin AM. Molecular and cellular mechanisms of osteoporosis. *Int J Mol Sci*. 2023;24(21):15772. doi: 10.3390/ijms242115772, PMID 37958752.
5. Jeong CH, Jeong HR, Kwak JH, Kim JH, Choi GN, Kim DO, et al. Phenolic composition and *in vitro* antioxidant activities of *Smilax china* Root. *J Food Biochem*. 2013;37(1):98-107. doi: 10.1111/j.1745-4514.2011.00610.x.
6. Song L, Tian L, Ma Y, Xie Y, Feng H, Qin F, et al. Protection of flavonoids from *Smilax china* L. rhizome on phenol mucilage-induced pelvic inflammation in rats by attenuating inflammation and fibrosis. *J Funct Foods*. 2017;28:194-204. doi: 10.1016/j.jff.2016.11.015.
7. Feng H, He Y, La L, Hou C, Song L, Yang Q, et al. The flavonoid-enriched extract from the root of *Smilax china* L. inhibits inflammatory responses via the TLR-4-mediated signaling pathway. *J Ethnopharmacol*. 2020;256:112785. doi: 10.1016/j.jep.2020.112785, PMID 32222576.
8. Ahmad HI, Shoab Khan HM, Akhtar N, Ijaz S. Phenolic, flavonoid content and radical scavenging activity of *Smilax china* with its inhibitory potential against clinically important enzymes. *Nat Prod Res*. 2021;35(12):2066-71. doi: 10.1080/14786419.2019.1648463, PMID 31385538.
9. Azizul NH, Hapidin H, Abdullah H, Azlan M, Ahmad A, Soelaiman IN. Potential effects of polyphenols on osteoblast and osteoclast culture. *Biomed Res Ther*. 2023;10(1):5476-90. doi: 10.15419/bmrat.v10i1.786.
10. Sharma AR, Lee YH, Bat-Ulzii A, Chatterjee S, Bhattacharya M, Chakraborty C, et al. Bioactivity, molecular mechanism, and targeted delivery of flavonoids for bone loss. *Nutrients*. 2023;15(4):919. doi: 10.3390/nu15040919, PMID 36839278.
11. Nguyen HT, Nguyen MT, Nguyen TX, Pham QM, Nguyen HX, Nguyen PT. Ethyl acetate extract of *Smilax glabra* Roxb roots and its major active compound astilbin promote osteoblastogenesis *in vitro* by upregulating bone cell differentiation-associated genes. *Asian Pac J Trop Biomed*. 2021;11(12):553-60. doi: 10.4103/2221-1691.331271.
12. Bhati R, Singh A, Anand V, et al. Pharmacognostical standardization, extraction and anti-diabetic activity of *Smilax china* L. rhizome. *Tradit Med*. 2011;6(5):218-23.
13. Zainab R, Akram M, Abbaass W. Pharmacological evaluation, phytochemical analysis and medicinal properties of *Smilax chinensis* D.C. *Asian Journal*. *Asian J Emerg Res*. 2019;1(2):57-61. doi: 10.3923/ajerp.2019.57.61.
14. Gangadasu AR, Jat R, Selvam P. Investigation of phytochemicals and Spectral data of aqueous, ethanolic, and methanolic extracts of *Smilax china*. 2022;7(5):88-105. doi: 10.35629/7781-070588105.
15. Iqbal MO, Gu Y, Khan IA, Wang R, Chen J. Evaluation of the *in vitro* antioxidant and antitumor activity of hydroalcoholic extract from *Jatropha mollissima* leaves in Wistar rats. *Front Chem*. 2023;11:1283618. doi: 10.3389/fchem.2023.1283618, PMID 38164252.
16. Mosmann T. Rapid colorimetric assay for cellular growth and survival: application to proliferation and cytotoxicity assays. *J Immunol Methods*. 1983;65(1-2):55-63. doi: 10.1016/0022-1759(83)90303-4, PMID 6606682.
17. Yuan YG, Zhang S, Hwang JY, Kong IK. Silver nanoparticles potentiates cytotoxicity and apoptotic potential of camptothecin in human cervical cancer cells. *Oxid Med Cell Longev*. 2018; 2018:6121328. doi: 10.1155/2018/6121328, PMID 30647812.
18. Chen X, Zhao X, Gao Y, Yin J, Bai M, Wang F. Green synthesis of gold nanoparticles using carrageenan oligosaccharide and their *in vitro* antitumor activity. *Mar Drugs*. 2018;16(8):277. doi: 10.3390/md16080277, PMID 30087223.
19. Mahendiran B, Muthusamy S, Janani G, Mandal BB, Rajendran S, Krishnakumar GS. Surface modification of decellularized natural cellulose scaffolds with organosilanes for bone tissue regeneration. *ACS Biomater Sci Eng*. 2022;8(5):2000-15. doi: 10.1021/acsbmaterials.1c01502, PMID 35452211.
20. Cheung EY, Tan KC, Cheung CL, Kung AW. Osteoporosis in East Asia: current issues in assessment and management. *Osteoporos Sarcopenia*. 2016;2(3):118-33. doi: 10.1016/j.afos.2016.07.001, PMID 30775478.
21. Vijayalakshmi A, Ravichandiran V, Anbu J, Velraj M, Jayakumari S. Anticonvulsant and neurotoxicity profile of the rhizome of *Smilax china* Linn. in mice. *Indian J Pharmacol*. 2011;43(1):27-30. doi: 10.4103/0253-7613.75662, PMID 21455417.
22. Changani H, Parikh P. Molecular insights for an anti-osteoporotic properties of *Litsea glutinosa* on Saos-2 cells: an *in vitro* approach. *J Ayurveda Integr Med*. 2022;13(2):100501. doi: 10.1016/j.jaim.2021.07.017, PMID 34799209.
23. Li N, Zhou L, Xie W, Zeng D, Cai D, Wang H, et al. Alkaline phosphatase enzyme-induced biomineralization of chitosan scaffolds with enhanced osteogenesis for bone tissue engineering. *Chem Eng J*. 2019;371:618-30. doi: 10.1016/j.cej.2019.04.017.
24. Zhang J, Liu Z, Luo Y, Li X, Huang G, Chen H, et al. The role of flavonoids in the osteogenic differentiation of mesenchymal stem cells. *Front Pharmacol*. 2022;13:849513. doi: 10.3389/fphar.2022.849513, PMID 35462886.
25. Wong SK, Chin KY, Ima-Nirwana S. Quercetin as an agent for protecting the bone: a review of the current evidence. *Int J Mol Sci*. 2020;21(17):6448. doi: 10.3390/ijms21176448, PMID 32899435.
26. Liu XW, Ma B, Zi Y, Xiang LB, Han TY. Effects of rutin on osteoblast MC3T3-E1 differentiation, ALP activity and Runx2 protein expression. *Eur J Histochem*. 2021;65(1):3195. doi: 10.4081/ejh.2021.3195, PMID 33478200.
27. Wong RW, Rabie AB. Effect of quercetin on bone formation. *J Orthop Res*. 2008;26(8):1061-6. doi: 10.1002/jor.20638, PMID 18383168.
28. Zhao B, Xiong Y, Zhang Y, Jia L, Zhang W, Xu X. Rutin promotes osteogenic differentiation of periodontal ligament stem cells through the GPR30-mediated

- PI3K/AKT/mTOR signaling pathway. *Exp Biol Med* (Maywood). 2020;245(6):552-61. doi: 10.1177/1535370220903463, PMID 32036685.
29. Triwardhani A, Patera NA, Hadianto L, *et al.* JMolecular Docking of Marumosiide, Rutin, and quercetin in *Moringa oleifera* to Bone Remodeling Biomarkers: an *in silico* study. *J Int Dent Med Res*. 2023: 995-1003.
30. Li D, Yin W, Xu C, Feng Y, Huang X, Hao J, *et al.* Rutin promotes osteogenic differentiation of mesenchymal stem cells (MSCs) by increasing ECM deposition and inhibiting p53 expression. *Aging*. 2024;16(4):3583-95. doi: 10.18632/aging.205546, PMID 38349887.

Cite this article: Makeen HA, Albratty M. *In silico* and *in vitro* Investigation of Osteogenesis Potentiality of *Smilax china* Hydro Alcoholic Root Extract on Human Osteoblast-like Cell Line (Saos2)-A Novel Approach. *Indian J of Pharmaceutical Education and Research*. 2026;60(2s):s805-s814.